Gene mapping and candidate gene analysis of a novel watermelon lesion mimic mutant *clalm*

wei dong
Henan University https://orcid.org/0000-0002-9377-0121
kai liu
Henan University
de feng wu
Henan University
Guo Jinggong (jgguo@henu.edu.cn)
Henan University

Research Article

Keywords: Watermelon, lesion mimic mutant, leaf spotting, whole genome resequencing–bulked segregant analysis, fatty acid amide hydrolase, RNAi

Posted Date: August 19th, 2021

DOI: https://doi.org/10.21203/rs.3.rs-734432/v1

Abstract

The leaf is an extremely important plant organ exhibiting a broad range of phenotypic variation. In watermelon (*Citrullus lanatus*), leaf spotting is a rare, valuable trait that can be used by breeders for selection at early growth stages. In this study, we tested a seven-generation family to determine the inheritance and genetic basis of this trait. As revealed by analysis of the lesion mimic mutant *clalm*, leaf spotting is controlled by a single dominant gene. Whole genome resequencing–bulked segregant analysis demonstrated that this gene is located on chromosome 4 from 3,760,000 bp to 7,440,000 bp, a region corresponding to a physical distance of 3.68 Mb encompassing approximately 72 annotated genes and eight non-synonymous coding SNPs. According to quantitative real-time PCR analysis, the expression level of *ClCG04G001930* was significantly lower in the *clalm* mutant than in normal watermelon. The predicted target gene, *ClCG04G001930*, encodes a fatty acid amide hydrolase protein that regulates a variety of neurobehavioral processes in animals. Twelve-five SNPs were identified in the *ClCG04G001930* gene of F_2 individuals of the *clalm mutant*. RNA interference of the *ClCG04G001930* gene, designated as *ClPAD4*, yielded transgenic lines whose leaves gradually developed chlorotic lesions over 3 weeks. Our results suggest that *ClPAD4* is the gene responsible for leaf spotting in the *clalm* mutant. Our findings may serve as a foundation for elucidating the mechanism underlying the spotted leaf trait and should be useful for marker-assisted selection breeding in watermelon.

Introduction

The leaf is an extremely important plant organ displaying a broad range of phenotypic variation. Many quantitative trait locus (QTLs) and genes related to leaf spotting have been detected or cloned in different crops. In rice, lesion mimic mutants (LMMs), such as *spl7*, *spl11*, *spl28*, *spl30* and *lmr*, exhibit small, reddish-brown lesions or spots that develop at leaf tips or bases and gradually spread on fully expanded leaves (Yamanouchi et al., 2002; Zeng et al., 2004; Qiao et al., 2010; Fekih et al., 2015; Ruan et al., 2019). In Arabidopsis, overexpression of UGT76D1, which plays an important role in SA homeostasis, results in a hypersensitive response (HR)-like lesion mimic phenotype (Lv et al., 2019). In birch, BpGH3.5, an early auxin-response factor regulating root elongation, gives rise to typical LMM characteristics and accelerates leaf senescence (Li et al., 2017). In switchgrass, co-silencing of methylenetetrahydrofolate reductase and caffeic acid O-methyltransferase results in a novel lesion-mimic leaf phenotype (Liu et al., 2017). In contrast to these findings, the genetic mechanism underlying the lesion-mimic leaf phenotype of watermelon (*Citrullus lanatus*) remains unknown.

The genome of watermelon ($2n = 2x = 22$) comprises 11 chromosomes and has an approximate size of 425 Mb. The annotated watermelon genome sequence, which was released in 2013, includes 23,440 predicted protein-coding genes and is thus suitable for next-generation sequencing to accelerate the identification of candidate genes controlling important agronomic traits in this species. Watermelon fruit shape, skin color, and rind stripe patterning have been previously investigated by bulked segregant analysis and next-generation sequencing technology (BSA-seq) (Kim et al., 2015; Dou et al., 2018; 2019). The objective of the present study was the identification of the *LMM* gene in the watermelon

lesion mimic mutant *clalm*. We re-sequenced the whole genome of two DNA bulks (i.e., spotted leaf and normal pools) developed from plants in an F_2 population. Our study results provide preliminary evidence that *ClCG04G001930* encoding lipase-like PAD4 is the responsible gene. To our knowledge, our study is the first reported gene mapping and elucidation of the inheritance mechanism controlling leaf spotting in watermelon. To improve the quality of watermelon cultivars, breeders have focused on the introduction of novel traits into existing germplasm. The application of the spotted leaf trait as a selection tool in breeding programs will thus help improve the ability of breeders to make selections at early growth stages, thus accelerating the watermelon breeding program.

Methods

Plant materials

Watermelon cultivars Zhengduanman (the wild type) and lesion mimic mutant *clalm* were self-pollinated for seven generations to obtain stable leaf spotting phenotypes. For use as research materials, 47 F_2 segregation populations (25+22 mixed pools with extreme characteristics), 20 parent plants, and inbred lines were grown and evaluated at the Henan University Genetics and Breeding Base in the spring of 2018.

Trypan blue staining

To analyze the state of lesion mimic leaf cells, leaves were incubated in fixative solution, immersed and rinsed five times in ultrapure water, and placed on filter paper. After absorption of excess water, the leaves were stained at room temperature for 2 to 6 h in darkness. Next, the leaves were immersed and rinsed five time in ultrapure water and then immersed and stored in plant trypan blue dye solution B for 3 to 16 h. After incubation for 30 min at room temperature in 20 ml of plant trypan blue dye solution, the leaves were photographed.

Microscopic observations

For light microscopic examination, leaves were fixed in fixative solution (4% paraformaldehyde) for 24 h and then dehydrated, embedded in paraffin, and sliced as previously described (O'Brien et al. 1964). The slices were stained with toluidine blue and sealed in neutral gum heated to 38°C. The prepared samples were observed with an Eclipse E100 microscope (Nikon, Tokyo, Japan) at 100 × magnification. For staining prior to transmission electron microscopy (TEM) examination, targeted fresh tissues were selected to minimize mechanical damage. Fresh tissue blocks (£ 1 mm^2) were quickly cut with a sharp blade and harvested within 1 to 3 min. The washed tissue blocks were immediately fixed with electron microscopy fixative for 2 h at room temperature and then transferred to 4°C for preservation and transportation.

Samples were fixed in a solution of 1% OsO_4 in PB (0.1 M, pH 7.4) for 7 h at room temperature. After removal of OsO_4, the tissues were rinsed three times in 0.1 M PB (pH 7.4), dehydrated in a graded ethanol

series (30%, 50%, 70%, 80%, 90%, 95%, and 100%) for 1 h at each concentration, resin penetrated, and embedded at 37°C in a graded reagent series (3:1 acetone:EMBed 812 for 2–4 h; 1:1 acetone:EMBed 812 overnight; 1:3 acetone:EMBed 812 for 2–4 h; and pure EMBed 812 for 5–8 h). Tissues were inserted into embedding molds filled with pure EMBed 812 resin and then incubated overnight in a 37°C oven. The embedding molds containing resin and samples were moved to a 65°C oven and allowed to polymerize for more than 48 h. The resin blocks were cut into 60- to 80-nm sections using an ultramicrotome, and the tissues were fished out onto 150-mesh cuprum grids with formvar film. The grid-attached tissues were stained with 2% uranium acetate-saturated alcohol solution in darkness for 8 min, rinsed three times each with 70% ethanol and ultrapure water, stained with 2.6% lead citrate in the absence of CO_2 for 8 min, and rinsed three times with ultrapure water. After blotting with filter paper, the cuprum grids were placed on a grid board and dried overnight at room temperature. The samples were examined under an HT7700 transmission electron microscope (Hitachi, Japan).

Sample collection and BSA library preparation

Young leaves of the parents and F_2 plants were collected and immediately placed in liquid nitrogen, and total genomic DNA was isolated using the CTAB method. Genomic DNA samples of 47 F_2 segregation populations and 20 parent plants were subjected to whole-genome resequencing performed by the Beijing Biomarker Technologies Corporation (Beijing, China). To generate bulked samples, equal amounts of DNA from each plant per group were mixed to form yellow-spot (Y-pool) and normal (N-pool) sets at a final concentration of 40 ng/μL. Prior to high-throughput sequencing, DNA samples were sonicated to produce 350-bp fragments. After trimming of barcodes, clean, high-quality reads from identical samples were mapped onto the *C. lanatus* subsp. *vulgaris* 'Charleston Gray' genome sequence (http://cucurbitgenomics.org/organism/4). All identified SNPs shared across the bulk were considered polymorphic in association studies. To represent the difference between the SNP index of the two pools, we calculated ΔSNP and ΔInDel indexes, which are association analysis metrics used to find significant differences in genotype frequency between two pools (Fekih et al. 2013; Hill et al., 2013). Candidate regions over the threshold (99th percentile) were extracted from each linkage group.

Expression analysis of candidate genes

We investigated the expression patterns of *ClCG04G000300*, *ClCG04G000420*, *ClCG04G001450*, *ClCG04G001740*, *ClCG04G001900*, and *ClCG04G001930* using qRT-PCR. Zhengduanman and Duanbanban seedlings were grown for 10, 30, and 60 days. Spotted leaves and normal leaves were collected from three plants each, and each sample collection was repeated three times. After addition of SYBR Green I to each reaction mixture, qRT-PCR amplifications were performed on a Roche LightCycler 480 II instrument using the following thermal profile: a 30-s hot start at 95°C followed by 40 cycles of 95°C for 5 s and 60°C for 30 s. The *ClYLS8* gene was included as a control for normalizing gene expression data (Dong et al., 2018). The primers used to amplify genes are listed in Table 1.

Bioinformatic analysis

The homology of nucleotide sequences of candidate gene was analyzed online (http://www.ncbi.nlm.nih.gov). A phylogenetic tree comprising the target gene and its homologous sequences was constructed using the MEGA 7.0 software (Kumar et al. 2001). A bootstrap analysis (1,000 replicates) was completed to assess the reliability of the tree (Felsenstein 1992). The high quality tree figure was created online (https://itol.embl.de/).

Watermelon transformation

The binary RNAi interference vectors DHpart27RNAi-FADP1P4 were constructed as described by Li et al. (2019). In brief, 300-bp target fragments of the candidate gene were inserted between Hind and XbaII sites in the vector, and the reverse sequence was inserted between XhoI and KpnI sites. The watermelon explants were transformed according to a modified method (Yu et al., 2011; Liu et al., 2016; Ren et al., 2018). In particular, surface-sterilized watermelon seeds of watermelon cultivars Kexi (the wild type) were sown on basic Murashige–Skoog solid medium supplemented with 3% Suc and maintained for 2 days in darkness and for 2 to 3 days under a 16-h/8-h light/dark photoperiod. The cotyledons were excised, and hypocotyls and the apical portion were discarded. *Agrobacterium tumefaciens* strain GV3101 harboring the binary vector was used for the transformation. The cotyledon explants were co-cultivated in darkness for 4 days. After transfer and maintenance on selective induction medium for 4 weeks, the explants were transferred onto selective elongation medium containing 0.2 mg/L KT, 60 mg/L Kan, and 400 mg/L Cef and incubated for 2 weeks. Plantlets with well-developed roots were taken from the rooting medium and placed in plastic cups containing vermiculite.

Determination of salicylic acid (SA) content

Fresh leaves (ca. 0.5 g) were homogenized in liquid nitrogen and transferred to a 1.5-mL centrifuge tube containing 0.5 mL of 90% methanol. The homogenate was centrifuged at 10,000 *g* for 15 min to obtain a supernatant. Next, 0.25 mL of 5% trichloroacetic acid was added to dissolve the precipitate, and 0.8 mL of a mixture of 1:1 (v/v) ethyl acetate and cyclohexane was added after shaking. The extraction was performed twice, with the upper organic phase transferred to a new centrifuge tube, and an additional 0.6 mL of the 1:1 ethyl acetate:cyclohexane solution was added for dissolution. After filtration through a 0.45-μm filter membrane, the samples were analyzed by HPLC.

Results

Morphology of lesion mimic mutant *clalm*

Plants of lesion mimic mutant *clalm* were self-pollinated for seven generations to yield stable yellow spotting on leaves and fruits. Yellow spots appeared on leaves 10 days after sowing and then gradually spread over entire leaves and fruits during the life cycle of lesion mimic mutant *clalm*, the female parent (Fig. 1a–d). All plants of the F_1 generation developed spotted leaves, whereas the ratio

of spotted- to non-spotted-leaf plants in the F_2 population conformed to a Mendelian segregation ratio of 3:1 (χ^2 £ 0.5, P <0.05).

Necrotic tissue of lesion mimic mutant *clalm* spotted-leaf

In contrast to living tissue, necrotic tissue can be stained with trypan blue. Dead leaf-membrane cells will appear dark blue, whereas other parts should be almost colorless. We therefore stained leaves of the wild type andlesion mimic mutant *clalm* with trypan blue, which revealed that leaves of lesion mimic mutant *clalm*, but not those of the wild type, harbored small, spontaneous lesions (Fig. 1e, f).

Microscopic observations

No significant differences between speckled leaf areas and normal leaves were observed under a light microscope (Fig. 2A a, B a). Obvious differences were detected, however, using TEM. First, mesophyll cells of normal leaves were rich in chloroplasts, whereas those of lesion mimic mutant *clalm* spotted leaves contained very little chlorophyll (Fig. 2A b, B b). Second, mesophyll cell chloroplasts of normal leaves were rich in starch grains, but starch grains were absent from those of spotted leaves (Fig. 2A c, B c). Finally, mesophyll cell chloroplasts of normal leaves were rich in grana; in contrast, those of spotted leaves had no grana and only a few thylakoids (Fig. 2A c, B c).

Whole-genome resequencing analysis

Filtering of 44.31 Gb of raw data yielded 43.89 G of clean data for further analysis. The Q30 ratio of the clean data was 85%, and the GC content was 41.67%, with an average genome resequencing depth of 22.75× and a genome coverage of 98.81%. The data have been submitted to the NCBI database (submission number: SUB10041505). Compared with the reference genome, 165,590 SNPs and 71,589 insertions–deletions (InDels) were identified between spotted- and non-spotted-leaf parents (Fig. 3). A Circos plot of the chromosomal distribution of candidate regions among samples is shown in Fig. 4. In addition, 12,784 SNPs and 19,212 InDels were found in the two bulk segregant populations. Association analyses between the two bulks based on SNP and InDel indexes narrowed the candidate region to approximately 4.04 Mb (Fig. 5a) and 4.00 Mb (Fig. 5b), respectively. Collectively, these two indexes indicated the candidate gene was located in an approximately 3.68-Mb region on chromosome 4 containing roughly 72 annotated genes and eight non-synonymous coding SNPs. These SNPs were likely directly associated with leaf spotting.

Identification of the *LMM* gene

We examined expression levels of six candidate genes (*ClCG04G000300*, *ClCG04G000420*, *ClCG04G001450*, *ClCG04G001740*, *ClCG04G001900*, and *ClCG04G001930*) in the two parental watermelon lines by qRT-PCR to assess whether their expression levels were correlated with the spotted leaf phenotype (Fig. 6). The expression level of *ClCG04G001930* was considerably higher

in Zhengduanman than in Duanbanban plants ($P < 0.05$), thus suggesting that this gene is responsible for leaf spotting in lesion mimic mutant *clalm*.

ClCG04G001930 was predicted to encode a lipase-like PAD4, a protein that plays an important regulatory role in leaf senescence in many plant species. We therefore hypothesized that *ClCG04G001930* is a *lipase-like PAD4* homolog in watermelon and accordingly named this gene *ClPAD4*. According to an amino acid sequence multiple alignment (Fig. 7a), the ClPAD4 protein is 100% similar to PAD4 proteins of *Cucumis sativus* (accession number XP_011653897.1), *Cucumis melo* (XP_008442139.1), *Cucurbita maxima* (XP_022966244.1), and *Momordica charantia* (XP_022149409.1). Twenty-five SNPs, one of which was a non-synonymous coding SNP, were identified in *ClCG04G001930* (Table 2). The constructed phylogenetic tree clarified the molecular evolutionary relationship between ClPAD4 and its homologs (Fig. 7b)

RNAi of *ClPAD4* in watermelon

To characterize the function of *ClPAD4*, we generated transgenic knockdown watermelon plants for this gene. We obtained 56 transgenic plants and screened them for positive clones (Fig. 8a). After 3 weeks, the regenerated shoots were transferred to rooting medium and grown for another 3 weeks, and chlorotic lesions gradually appeared on leaves (Fig. 8b). The rooted shoots were transferred to plastic cups containing vermiculite. Twelve individual kanamycin-resistant plants were obtained after acclimation and had obvious chlorotic lesions on leaves (Fig. 8c, d). The leaves of transgenic plants and *clalm* stained with trypan blue exhibited small, spontaneous lesions (Fig. 9a, b). RNAi of *ClPAD4* in watermelon thus produced obvious leaf spotting.

SA content

We used HPLC to compare the SA content of leaves of different watermelon lines. According to HPLC analysis, the leaf SA content of lesion mimic mutant *clalm* was lower than that of Zhengduanman and higher than that of the transgenic plants (Fig. 9d).

Discussion

The strategy used by watermelon breeders to improve the quality of watermelon cultivars is the introduction of novel traits, especially ones useful for seedling screening, into existing germplasm. The underlying gene in lesion mimic mutants of watermelon and other cucurbitaceous crops has not yet been well studied.

The timing of spot appearance can be used to circumscribe vegetative, reproductive, and complete growth periods (Qiao et al., 2010; Ma et al 2019). In our study, yellow spots emerged on watermelon cotyledons 10 days after sowing, which makes their presence an obvious marker for identifying impure and aberrant varieties at the seedling stage. The seedlings grow very slowly and flowered late, which was consistent with previous reports. In rice lesion mimic mutants, leaf spots appear

during the seedling stage and are relatively weakly correlated with the duration of the entire growth period (Zhang et al. 2018). We found that watermelon lesion mimicry is controlled by a single dominant gene. Lesion mimic mutants (LMMs) are relatively rare in cucurbitaceous species, with the spotting trait mainly manifested in fruits and seeds. In addition, a single dominant gene is responsible for fruit spotting in non-spotted varieties of *Cucumis melo*, *Cucurbita pepo*, and watermelon (Paris et al., 2000; 2002; Ntui and Uyoh 2005; Pitrat 2002; Lv et al., 2018). In rice, a single dominant gene controls the LMM phenotype of *NH1*, *spl12*, *spl13*, *spl15*, and *spl24* mutants, whose leaves display small, reddish-brown lesions or spots (Mizobuchi et al., 2002; Yuan et al., 2007; Wu et al., 2008). Many LMMs exhibit altered disease resistance and are thus considered ideal for studying signaling pathways in species such as Arabidopsis, maize, and rice (Johal et al., 1995; Lorrain et al., 2004; Shirsekar et al., 2014; Wang et al., 2015; Wang et al., 2017).

Watermelon *LMM* genes are valuable experimental materials for studying molecular mechanisms and creating new germplasm resources. The advent of BSA-seq has accelerated the identification of candidate genes controlling important agronomic traits (Dong et al., 2018; Lv et al., 2018). This method has been used to map major QTLs for powdery mildew resistance to chromosome 12 in melon (Li et al., 2017). In addition, the candidate genes *Csa2M435460.1* and *Csa5M579560.1* conferring resistance to cucumber powdery mildew have been identified using BSA-seq (Xu et al., 2016). Furthermore, a genome-wide analysis of SNPs resulted in the detection of a genomic region harboring the candidate dwarfism gene *Cla010726* (Dong et al., 2018). In contrast, few researchers have investigated the gene responsible for spontaneous lesion mimicry in watermelon and other cucurbitaceous crops. In this study, we used BSA-seq to map *ClCG04G001930* of watermelon for the first time. We localized this gene to chromosome 4 in a region between 3,760,000 bp to 7,440,000 bp, corresponding to a physical distance of 3.68 Mb. *ClCG04G001930* is a *PAD4* homolog in watermelon. ClPAD4 and AtPAD4 have a protein sequence similarity of 62.72%, which suggests that they have similar functions (Fig. 7). PAD4 orthologs are present in many plant species and are essential for systemic resistance against biotic stress in angiosperms (Rusterucci et al. 2001; Gao et al. 2014; ke et al. 2014; Yan et al. 2016; Chen et al. 2018). AtPAD4 is a member of a small family of sequence-related immunity regulators (Feys et al. 2005; Lapin et al. 2019). Heterologous expression of the *AtPAD4* gene in soybean roots inhibits the development of plant parasitic nematodes. GbPAD4 is up-regulated in cotton during pathogen infection (Zhang et al. 2012), and LePAD4 expression is elevated in response to green peach aphid infestation in tomato (Singh et al. 2012). The PAD4 protein in grape supports the response of the SA defense pathway to biotic stress (Tandon et al. 2015). ICS1, NPR1-3, PRs, EDS1, PAD4, and FMO1 signaling is strongly elicited during rust disease infection in rice (Sahu et al. 2020).

PAD4 is involved in the regulation of programmed cell death and acclimation to biotic and abiotic stresses (Yan et al. 2016; Chen et al. 2018). We detected an obvious difference between LMM and normal watermelon leaves under an electron microscope: the cells of watermelon LMM leaves contained very little chlorophyll, whereas those of normal leaves were rich in chloroplasts and grana (Fig. 2a, b). Chloroplasts play an important role in regulating PAD4-modulated stress responses (Mühlenbock et al., 2008; Karpi ´nski et al., 2013; Bernacki et al., 2019). Our experimental result is thus very interesting and

requires detailed study. Cotyledons of the transgenic *clpad4* watermelon plants exhibited spontaneous lesions (Fig. 8d). Previous studies have shown that the LMM phenotype of the mutant *cpr5* is controlled by PAD4-dependent SA accumulation (Jirage et al. 2001; Lorrain et al. 2004). Silencing of OsPAD4 increases sensitivity to biotrophic pathogens in rice (Ke et al. 2014), and silencing of GmPAD4 reduces SA accumulation and enhances soybean susceptibility to virulent pathogens (Wang et al. 2014). SA is a plant endogenous hormone that participates in the regulation of physiological processes related to plant growth and development, including growth, maturity, and senescence, which plays an important role as a signal molecule in plant signal transduction and stress resistance. The SA content of transgenic and lesion mimic mutant *clalm* leaves was less than that of Kexi (Fig. 9d). Our experimental results, which are consistent with previous studies, indicate that the mutation of *ClPAD4* in watermelon most likely affected the accumulation of SA and ultimately led to the spontaneous lesions.

Genes used as screening markers for resistance breeding, biomass production, and productivity enhancement are important from an agricultural point of view. Watermelon breeders have always focused on the introduction of novel traits into existing germplasm as a means of improving cultivar quality. Cotyledons of *ClPAD4* RNAi transgenic watermelons exhibited obvious chlorotic lesions, which makes this application useful for seedling screening. Future elucidation of the mechanism of the *PAD4* gene with respect to the spotted leaf trait should be useful in molecular marker-assisted selection breeding of watermelon.

Declarations

Funding information

This work was supported by funding from the National Natural Science Foundation of China (31801882) and Henan Province Key Science and Technology Projects (212102110044 and 192102310024).

Author contributions

WD and JGG jointly designed all experiments. WD wrote the manuscript. WD and KL grew the plant materials and recorded the morphological characteristics. WD and DFW completed the whole-genome resequencing analysis and the molecular experiments. All authors contributed to the article and approved the submitted version.

Conflicts of interest/Competing interests

The authors declare that they have no competing interests.

Availability of data and material

The data have been submitted to the NCBI database (submission number: SUB10041505).

Key message

ClPAD4 is the gene responsible for leaf spotting in the *clalm* mutant, which should be useful for marker-assisted selection breeding in watermelon at early growth stages.

References

BernackiM,Czarnocka W, Szechy ´nska-Hebda M, Mittler R, Karpi ´nski S (2019) Biotechnological Potential of LSD1, EDS1, and PAD4 in the Improvement of Crops and Industrial Plants. *Plants* 8(8):290. doi.org/10.3390/plants8080290

Chen G, Wei B, Li G, Gong C, Fan R, Zhang X (2018) TaEDS1 genes positively regulate resistance to powdery mildew in wheat. *Plant Mol Biol* 96(6):607-625. doi: 10.1007/s11103-018-0718-9.

Dong W, Wu D, Li G, Wu D, Wang Z (2018) Next-generation sequencing from bulked segregant analysis identifies a dwarfism gene in watermelon. *Sci Rep* 8(1):2908. doi: 10.1038/s41598-018-21293-1.

Dou J, Lu X, Ali A, Zhao S, Zhang L, He N, Liu W (2018) Genetic mapping reveals a marker for yellow skin in watermelon (*Citrullus lanatus* L.). *PLoS One* 13(9):e0200617. doi: 10.1371/journal.pone.0200617.

Dou J, Zhao S, Lu X, He N, Zhang L, Ali A, Kuang H, Liu W (2018) Genetic mapping reveals a candidate gene (ClFS1) for fruit shape in watermelon (*Citrullus lanatus* L.). *Theor Appl Genet* 131(4):947-958. doi: 10.1007/s00122-018-3050-5.

Fekih R, Takagi H, Tamiru M, Abe A, Natsume S, Yaegashi H, Sharma S, Sharma S, Kanzaki H, Matsumura H, Saitoh H, Mitsuoka C, Utsushi H, Uemura A, Kanzaki E, Kosugi S, Yoshida K, Cano L, Kamoun S, Terauchi R (2013) MutMap^{+}: Genetic Mapping and Mutant Identification without Crossing in Rice. *PLoS One* 8(7):e68529. doi: 10.1371/journal.pone.0068529.

Fekih R, Tamiru M, Kanzaki H, Abe A, Yoshida K, Kanzaki E, Saitoh H, Takagi H, Natsume S, Undan JR, Undan J, Terauchi R (2015) The rice (*Oryza sativa* L.) LESION MIMIC ESEMBLING, which encodes an AAA-type ATPase, is implicated in defense response. *Mol Genet Genemics* 290(2): 611-622. doi: 10.1007/s00438-014-0944-z.

Feys BJ, Wiermer M, Bhat RA, Moisan LJ, Medina-Escobar N, Neu C, Cabral A, Parker JE (2005) Arabidopsis SENESCENCE-ASSOCIATED GENE101 stabilizes and signals within an ENHANCED DISEASE SUSCEPTIBILITY1 complex in plant innate immunity. *Plant Cell* 17(9):2601-13. doi: 10.1105/tpc.105.033910.

Gao F, Dai R, Pike SM, Qiu W, Gassmann W (2014) Functions of EDS1-like and PAD4 genes in grapevine defenses against powdery mildew. *Plant Mol Biol* 86(4-5):381-393. doi: 10.1007/s11103-014-0235-4.

Hill JT, Demarest BL, Bisgrove BW, Gorsi B, Su YC, Yost HJ (2013) MMAPPR: Mutation Mapping Analysis Pipeline for Pooled RNA-seq. *Genome Res* 23 (4): 687-697. doi: 10.1101/gr.146936.112.

Johal GS, Hulbert S, Briggs SP (1995) Disease lesion mimics of maize: a model for cell death in plants. *BioEssays* 17(8):685-692. doi:10.1002/bies.950170805.

Jirage D, Zhou N, Cooper B, Clarke JD, Dong X, Glazebrook J (2001) Constitutive salicylic acid-dependent signaling in cpr1 and cpr6 mutants requires PAD4. *Plant J* 26(4): 395-407. doi: 10.1046/j.1365-313x.2001.2641040.x.

Karpi ´nski S, Szechy ´nska-Hebda M, Wituszy ´nska W, Burdiak P (2013) Light acclimation, retrograde signalling, cell death and immune defences in plants. *Plant Cell Environ* 36(4):736-744. doi: 10.1111/pce.12018.

Ke Y, Liu H, Li X, Xiao J, Wang S (2014) Rice OsPAD4 functions differently from Arabidopsis AtPAD4 in host-pathogen interactions. *Plant J* 78(4):619-631. doi: 10.1111/tpj.12500.

Kim H, Han D, Kang J, et al (2015) Sequence-characterized amplified polymorphism markers for selecting rind stripe pattern in watermelon (*Citrullus lanatus* L.). *Hortic Environ Biote* 56(3):341-349. doi:10.1007/s13580-015-0017-1.

Kumar S, Tamura K, Jakobsen IB, Nei M (2001) MEGA2: molecular evolutionary genetics analysis software. *Bioinformatics* 17(12):1244-1245. doi:10.1093/bioinformatics/17.12.1244.

Lapin D, Kovacova V, Sun X, Dongus JA, Bhandari D, Born P, Bautor J, Guarneri N, Rzemieniewski J, Stuttmann J, Beyer A, Parker J E (2019) A Coevolved EDS1-SAG101-NRG1 Module Mediates Cell

Death Signaling by TIR-Domain Immune Receptors. *Plant Cell* 31(10):2430-2455. doi: 10.1105/tpc.19.00118.

Li B, Zhao Y, Zhu Q, Zhang Z, Fan C, Luan F, Gao P (2017) Melon powdery mildew resistance gene location and candidate gene analysis. *China vegetables* 2017(6):17-24.

Li S, Li M, Li Z, Zhu Y, Ding H, Fan X, Li F, Wang Z (2019) Effects of the silencing of CmMET1 by RNA interference in chrysanthemum (*Chrysanthemum morifolium*). *Plant Biotechnol Rep* 13(4):63-72. doi: 10.1007/s11816-019-00516-5.

Li R, Chen S, Liu G, Han R, Jiang J (2017) Characterization and Identification of a woody lesion mimic mutant lmd, showing defence response and resistance to Alternaria alternate in birch. *Sci Rep* 7(1):11308. doi: 10.1038/s41598-017-11748-2.

Liu L, Gu Q, Ijaz R, Zhang J, Ye Z (2016) Generation of transgenic watermelon resistance to Cucumber mosaicvirus facilitated by an effective Agrobacterium-mediatedtransformation method. *Sci Hortic* 205:32-38. doi:org/10.1016/j.scienta.2016.04.013.

Liu S, Fu C, Gou J, Sun L, Huhman D, Zhang Y, Wang ZY (2017) Simultaneous Downregulation of MTHFR and COMT in Switchgrass Affects Plant Performance and Induces Lesion-Mimic Cell Death. *Front Plant Sci* 8:982. doi: 10.3389/fpls.2017.00982.

Lorrain S, Lin B, Auriac MC, Kroj T, Saindrenan P, Nicole M, Balagué C, Roby D (2004) Vascular associated death1, a novel GRAM domain-containing protein, is a regulator of cell death and defense responses in vascular tissues. *Plant Cell* 16(8):2217-2232. doi:10.1105/tpc.104.022038.

Lv J, Fu Q, Lai Y, Zhou M, Wang H (2018) Inheritance and gene mapping of spotted to non-spotted trait gene CmSp-1 in melon (Cucumis melo L. var. chinensis Pangalo). *Mol Breeding* 38:105. doi:10.1007/s11032-018-0860-8.

Lv R, Li Z, Li M, Dogra V, Lv S, Liu R, Lee KP, Kim C (2019) Uncoupled Expression of Nuclear and Plastid Photosynthesis-Associated Genes Contributes to Cell Death in a Lesion Mimic Mutant. *Plant Cell* 31(1):210-230. doi: 10.1105/tpc.18.00813.

Ma J, Wang Y, Ma X, Meng L, Jing R, Wang F, Wang S, Cheng Z, Zhang X, Jiang L, Wang J, Wang J, Zhao Z, Guo X, Lin Q, Wu F, Zhu S, Wu C, Ren Y, Lei C, Zhai H, Wan J (2019) Affiliations expandDisruption of gene SPL35, encoding a novel CUE domain-containing protein, leads to cell death and enhanced disease response in rice. Plant Biotechnol J 17(8):1679-1693. doi: 10.1111/pbi.13093.

Mizobuchi R, Hirabayashi H, Kaji R, Nishizawa Y, Yoshimura A, Satoh H, Ogawa T, Okamoto M (2002) Isolation and characterization of rice lesion mimic mutants with enhanced resistance to rice blast and bacterial blight. *Plant Sci* 163: 345-353. doi: 10.1016/S0168-9452(02)00134-6.

Mühlenbock P, Szechynska-Hebda M, Płaszczyca M, Baudo M, Mateo A, Mullineaux PM, Parker JE, Karpinska B, Karpinski S (2008) Chloroplast signaling and LESION SIMULATING DISEASE1 regulate crosstalk between light acclimation and immunity in Arabidopsis. *Plant Cell* 20(9):2339-2356. doi:10.1105/tpc.108.059618.

Ntui V and Uyoh E (2005) Inheritance of stripe pattern on fruits and seed colour in Begusi melon, Colocynthis citrullus L. *Glob J Agric Sci* 4(1):29-32. doi:10.4314/gjass.v4i1.2251.

Paris HS (2000) Gene for broad, contiguous dark stripes in cocozelle squash (Cucurbita pepo). *Euphytica* 115(3):191-196. doi:10.1023/A:1004074618717.

Paris HS (2002) Genetic control of irregular striping, a new phenotype in Cucurbita pepo. *Euphytica* 129(1):119-126. doi:10.1023/A:1021564610029.

Pitrat M (2002) 2002 gene list for melon. *Cucurb Genet Coop Rep*. 25:1-18.

Qiao Y, Jiang W, Lee JH, Park B, Choi MS, Piao R, Woo MO, Roh JH, Han L, Paek NC, Seo HS, Koh HJ. (2010) SPL28 encodes a clathrin-associated adaptor protein complex 1, medium subunit μ1

(AP1M1) and is responsible for spooted leaf and early senescence in rice (*Oryza sativa*). *New Phytol* 185(1): 258-274. doi:10.1111/j.1469-8137.2009.03047.x.

Ren Y, Guo S, Zhang J, He H, Sun H, Tian S, Gong G, Zhang H, Levi A, Tadmor Y, Xu Y (2018) A Tonoplast Sugar Transporter Underlies a Sugar Accumulation QTL in Watermelon. *Plant Physiol* 176(1):836-850. doi: 10.1104/pp.17.01290.

Ruan B, Hua Z, Zhao J, Zhang B, Ren D, Liu C, Yang S, Zhang A, Jiang H, Yu H, Hu J, Zhu L, Chen G, Shen L, Dong G, Zhang G, Zeng D, Guo L, Qian Q, Gao Z (2019) OsACL-A2 negatively regulates cell death and disease resistance in rice. *Plant Biotechnol J* 17(7):1344-1356. doi: 10.1111/pbi.13058.

Rusterucci C, Aviv DH, Holt BF 3rd, Dangl JL, Parker JE (2001) The disease resistance signalling components EDS1 and PAD4 are essential regulators of the cell death pathway controlled by LSD1 in Arabidopsis. *Plant Cell* 13(10):2211-2224. doi: 10.1105/tpc.010085.

Sahu R, Prabhakaran N, Kundu P, Kumar A (2021) Differential response of phytohormone signalling network determines nonhost resistance in rice during wheat stem rust (Puccinia graminis f. sp. tritici) colonization. *Plant Pathology* doi: 10.1111/ppa.13376

Shirsekar GS, Vega-Sanchez ME, Bordeos A, Baraoidan M, Swisshelm A, Fan J, Park CH, Leung H, Wang GL (2014) Identification and characterization of suppressor mutants of *spl11*-mediated cell death in rice. *Mol Plant Microbe In* 27(6):528-536.

Singh V and Shah J (2012) Tomato responds to green peach aphid infestation with the activation of trehalose metabolism and starch accumulation. *Plant Signal Behav* 7(6):605-607. doi: 10.4161/psb.20066.

Tandon G, Jaiswal S, Iquebal MA, Kumar S, Kaur S, Rai A, Kumar D (2015) Evidence of salicylic acid pathway with EDS1 and PAD4 proteins by molecular dynamics simulation for grape improvement. *J Biomol Struct Dyn* 33(10):2180-2191. doi: 10.1080/07391102.2014.996187.

Wang C, Zhang X, Fan Y, Gao Y, Zhu Q, Zheng C, Qin T, Li Y, Che J, Zhang M, Yang B, Liu Y, Zhao K (2015) XA23 is an executor R protein and confers broad-spectrum disease resistance in rice. *Mol Plant* 8: 290-302. doi: 10.1016/j.molp.2014.10.010.

Wang J, Shine MB, Gao QM, Navarre D, Jiang W, Liu C, Chen Q, Hu G, Kachroo A (2014) Enhanced disease susceptibility1 mediates pathogen resistance and virulence function of a bacterial effector in soybean. *Plant Physiol* 165(3):1269-1284.

Wang S, Lei C, Wang J, Ma J, Tang S, Wang C, Zhao K, Tian P, Zhang H, Qi C, Cheng Z, Zhang X, Guo X, Liu L, Wu C, Wan J (2017) SPL33, encoding an eEF1A-like protein, negatively regulates cell death and defense responses in rice. *J Exp Bot* 68(5): 899-913. doi: 10.1093/jxb/erx001.

Wu C, Bordeos A, Madamba MR, Baraoidan M, Ramos M, Wang GL, Leach JE, Leung H (2008) Rice lesion mimic mutants with enhanced resistance to diseases. *Mol Genet Genomics* 279(6):605-619. doi: 10.1007/s00438-008-0337-2.

Xu Q, Yang S, Yu T, Xu X, Yan Y, Qi X, Chen X (2016) Wholegenome resequencing of a cucumber chromosome segment substitution line and its recurrent parent to identify candidate genes governing powdery mildew resistance. *PLoS One* 11(10):e0164469. doi: 10.1371/journal.pone.0164469.

Yamanouchi U, Yano M, Lin HX, Ashikari M, Yamada K (2002) A rice spotted leaf gene, spl7, encodes a heat shock transcription factor protein. *Proc Natl Acad Sci USA* 99(11): 7531-7535. doi: 10.1073/pnas.112209199.

Yan Z, Xingfen W, Wei R, Jun Y, Zhiying M (2016) Island cotton enhanced disease susceptibility 1 gene encoding a lipase-like protein plays a crucial role in response to Verticillium dahliae by regulating the SA level and H2O2 accumulation. *Front Plant Sci* 7:1830. doi: 10.3389/fpls.2016.01830.

Yuan Y, Zhong S, Li Q, Zhu Z, Lou Y, Wang L, Wang J, Wang M, Li Q, Yang D, He Z (2007) Functional analysis of rice NPR1-like genes reveals that Os NPR1/NHI is the rice orthologue conferring disease resistance with enhanced herbivore susceptibility. *Plant Biotechno J* 5(2): 313-324. doi: 10.1111/j.1467-7652.2007.00243.x.

Yu TA, Chiang CH, Wu HW, Li CM, Yang CF, Chen JH, Chen YW, Yeh SD (2011) Generation of transgenic watermelon resistant to Zucchini yellow mosaicvirus and Papaya ringspot virus type W. *Plant Cell Rep* 30 (3):359-371. doi: 10.1007/s00299-010-0951-4.

Zeng LR, Qu S, Bordeos A, Yang C, Baraoidan M, Yan H, Xie Q, Nahm BH, Leung H, Wang GL (2004) Spotted leaf 11, a negative regulator of plant cell death and defense, encodes a U-box/armadillo repeat protein endowed with E3 ubiquitin ligase activity. *Plant Cell* 16(10): 2795-2808. doi: 10.1105/tpc.104.025171.

Zhang XB, Feng BH, Wang HM, Xu X, Shi YF, He Y, Chen Z, Sathe AP, Shi L, Wu JL (2018) A

substitution mutation in Os PELOTA confers bacterial blight resistance by activating the salicylic acid

pathway. *J Integr Plant Biol* 60(2):160-172. doi: 10.1111/jipb.12613.

Zhang B, Yang Y, Chen T, Yu W, Liu T, Li H, Fan X, Ren Y, Shen D, Liu L, Dou D, Chang Y (2012) Island cotton Gbve1 gene encoding a receptor-like protein confers resistance to both defoliating and non-defoliating isolates of Verticillium dahliae. *PloS One* 7(12):e51091. doi: 10.1371/journal.pone.0051091.

Tables

Table 1 Sequences of primers used for quantitative real-time PCR

Primer name	Forward primer sequence	Reverse primer sequence
ClCG04G000300	ACATCATCATCCTCCTCTTCC	ACAATCTTCTTCAGGTTTCCA
ClCG04G000420	AGTAAATGGAGGCTCAATGTCGT	CTGAATCTTCCGATGCAGAGTAC
ClCG04G001450	GCAAGTTGATTCCCGTGGT	TGGATGGTCCCTTTGTGTT
ClCG04G001740	CGTTGGGATGGTAGGGATA	GGAAAACAAAGTTTGGGCA
ClCG04G001900	TTCCAATATCAATCCCACCAGT	AGAATCTCCCAGACCCACCAAG
ClCG04G001930	TTCACCACAGAGTGTCTTCCTA	GTGTTTGTCCTATTCTCCTTGC
ClYLS8	AGAACGGCTTGTGGTCATTC	GAGGCCAACACTTCATCCAT

Table 2 Chromosomal positions and codons of 20 identified SNPs in *ClPAD4*.

Chr	Pos	Alt	Ref	Effect
CG_Chr04	6813880	G	A	UPSTREAM
CG_Chr04	6814479	A	T	UPSTREAM
CG_Chr04	6815120	A	G	UPSTREAM
CG_Chr04	6815495	C	G	UPSTREAM
CG_Chr04	6815780	T	A	UPSTREAM
CG_Chr04	6816047	T	G	SYNONYMOUS_CODING
CG_Chr04	6817020	G	T	INTRON
CG_Chr04	6817183	A	C	INTRON
CG_Chr04	6817562	G	A	INTRON
CG_Chr04	6817731	T	C	INTRON
CG_Chr04	6818525	T	C	INTRON
CG_Chr04	6818765	G	T	INTRON
CG_Chr04	6818849	C	T	INTRON
CG_Chr04	6819193	C	T	INTRON
CG_Chr04	6819271	A	G	INTRON
CG_Chr04	6820247	T	G	INTRON
CG_Chr04	6820404	T	A	INTRON
CG_Chr04	6820421	A	G	INTRON
CG_Chr04	6820559	C	A	INTRON
CG_Chr04	6820771	A	G	INTRON
CG_Chr04	6821891	T	A,C	INTRON
CG_Chr04	6822521	T	A	INTRON
CG_Chr04	6822827	T	G	INTRON
CG_Chr04	6823382	A	C	SYNONYMOUS_CODING
CG_Chr04	6823753	A	G	NON_SYNONYMOUS_CODING

Figures

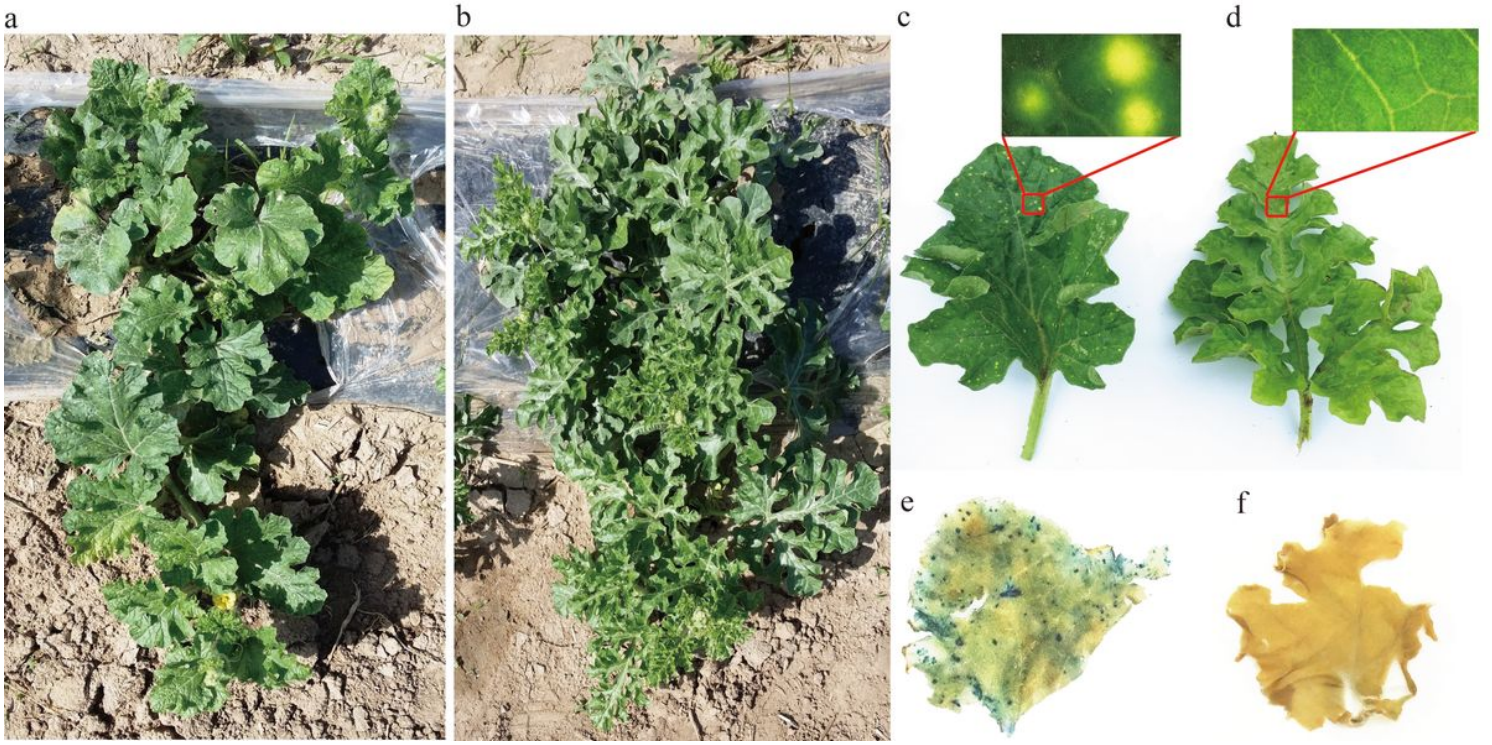

Figure 1

Comparative morphology of lesion mimic mutant clalm and wild-type Zhengduanman watermelon. (a–b) Plants of lesion mimic mutant clalm (a) and Zhengduanman (b) growing at the experimental breeding site. (c) Spotted leaf of lesion mimic mutant clalm. (d) Non-spotted leaf of Zhengduanman. (e–f) Leaves of lesion mimic mutant clalm (e) and Zhengduanman (f) stained with trypan blue.

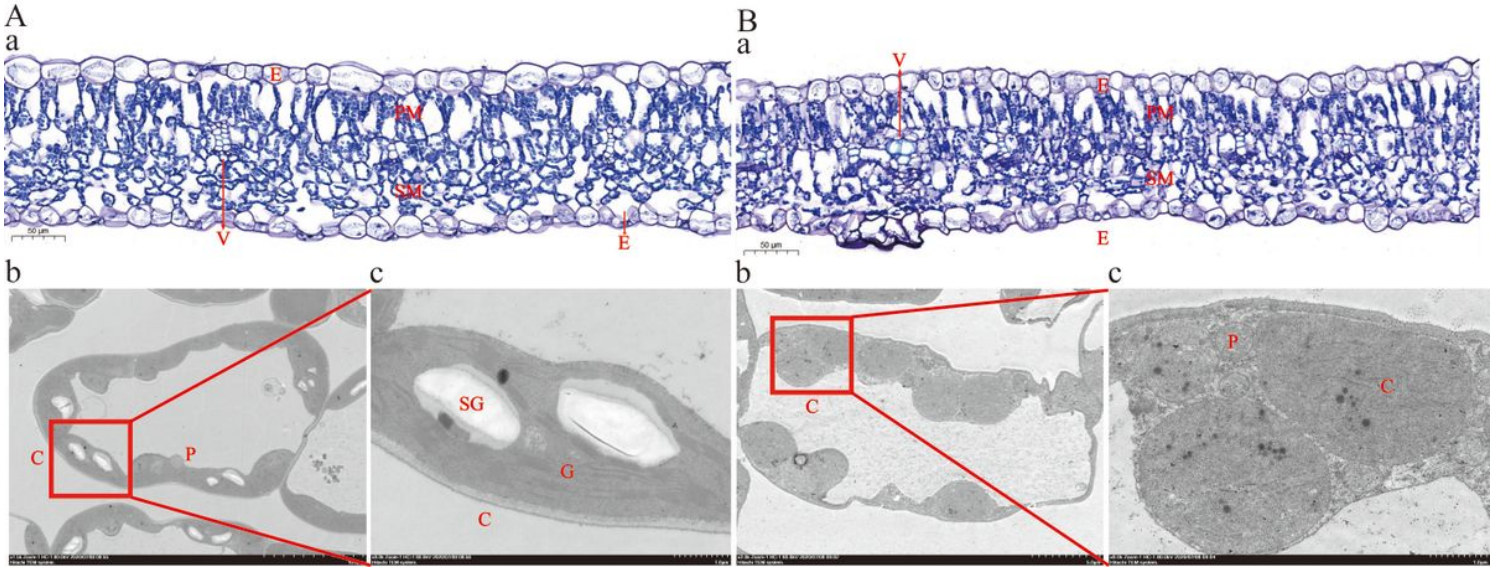

Figure 2

Microscopic images of lesion mimic mutant clalm (a) and wild-type Zhengduanman (b) leaf cross sections. E, epidermis; PM, palisade mesophyll cells; SM, spongy mesophyll cells; S, stoma; V, vein; C, chloroplasts; A, amyloplasts; P, peroxisome; SG, starch grain.

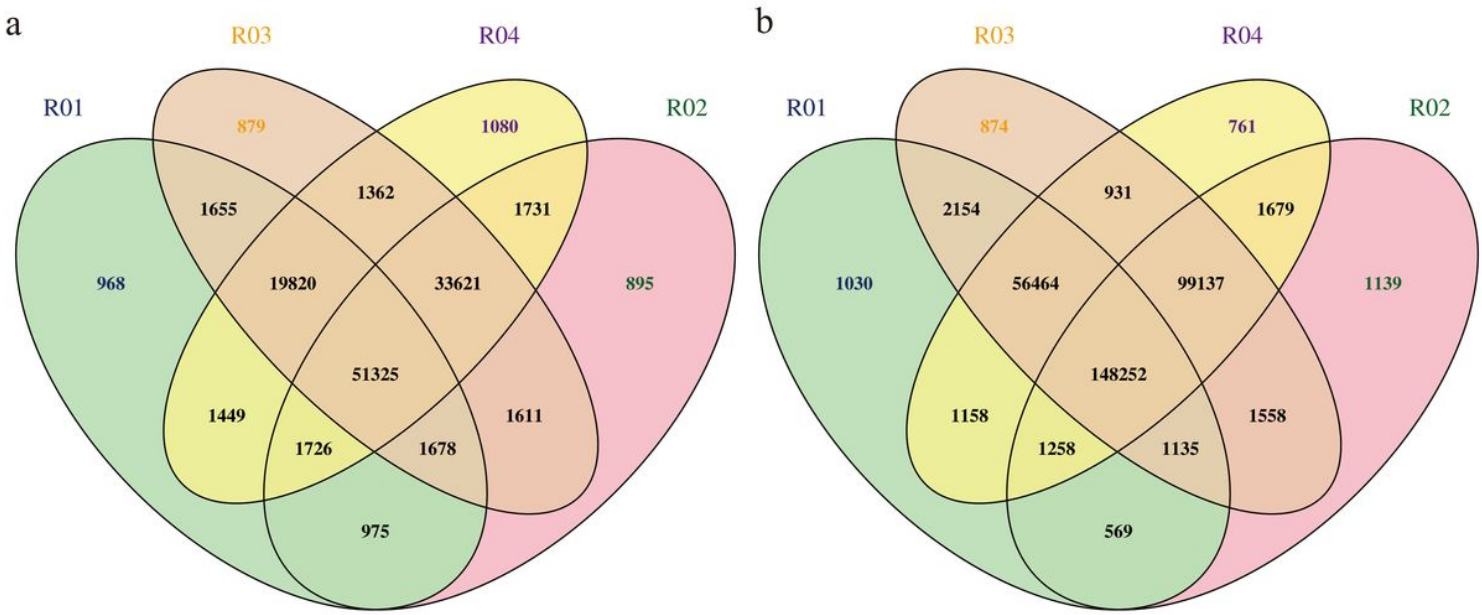

Figure 3

Venn diagrams of small InDels (a) and SNPs (b) in spotted-leaf and non-spotted-leaf watermelon.

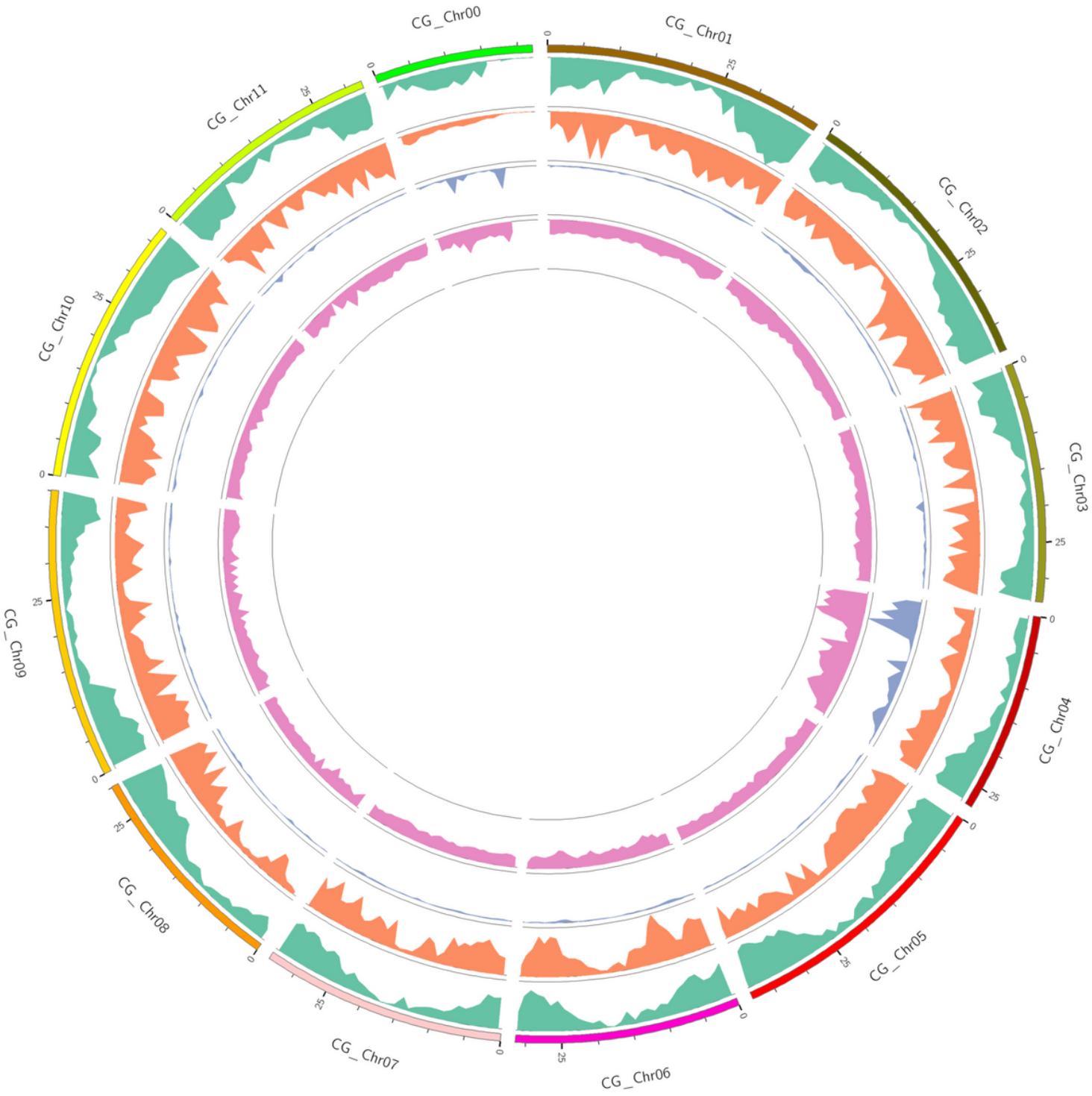

Figure 4

Circos plot of the chromosomal distribution of candidate regions among watermelon samples. Proceeding from the outside to the inside, the circles indicate (1) chromosomal coordinates and the distributions of (2) genes, (3) SNP densities, (4) ED values, and (5) ΔSNP index values.

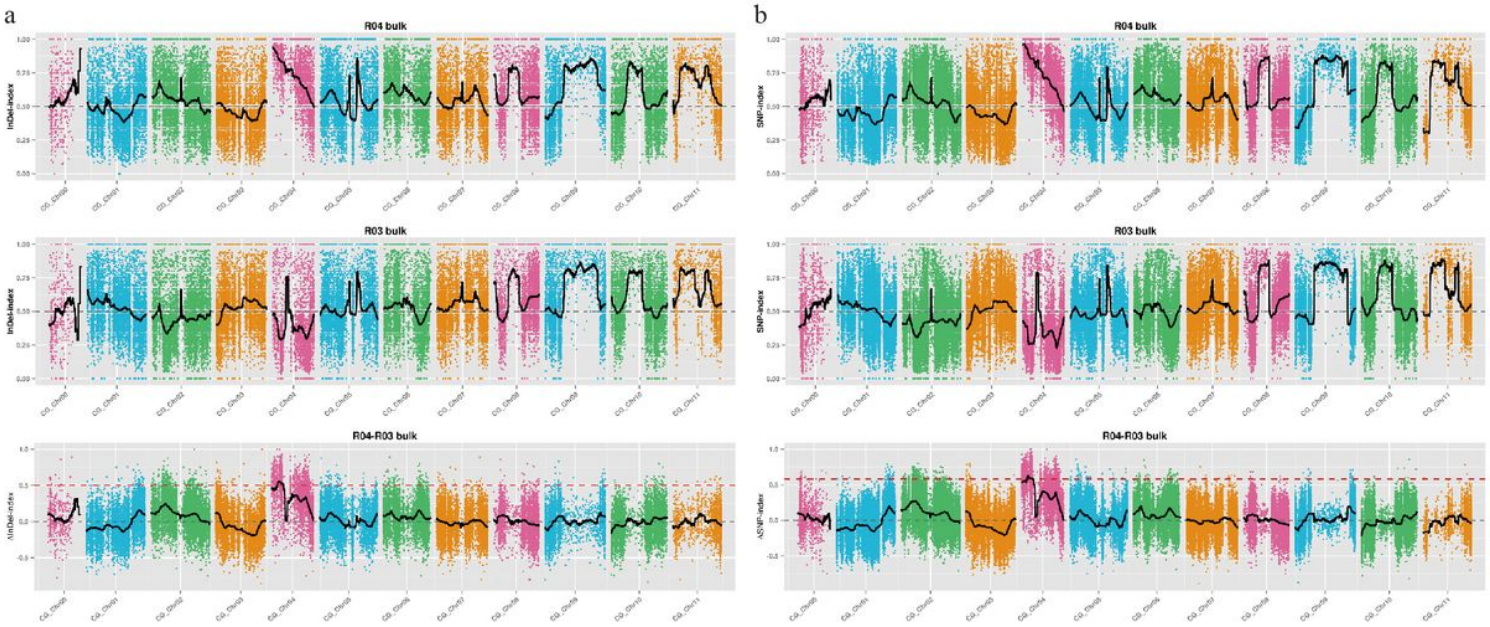

Figure 5

Chromosomal distributions of SNP, ΔSNP, InDel, and ΔInDel index values. (a) Chromosomal distributions of SNP index values in the non-spotted-leaf plant bulk from the F2 population (top), SNP index values in the spotted-leaf bulk from the F2 population (middle), and the difference in SNP index values (ΔSNP) between the two bulks (bottom). (b) Distributions of InDel index values in the non-spotted-leaf plant bulk from the F2 population (top), InDel index values of the spotted-leaf bulk from the F2 population (middle), and ΔIndel index values between the two bulks (bottom). The 99% threshold in each figure is indicated by a red dashed line, and Citrullus lanatus chromosome numbers are shown at the bottom.

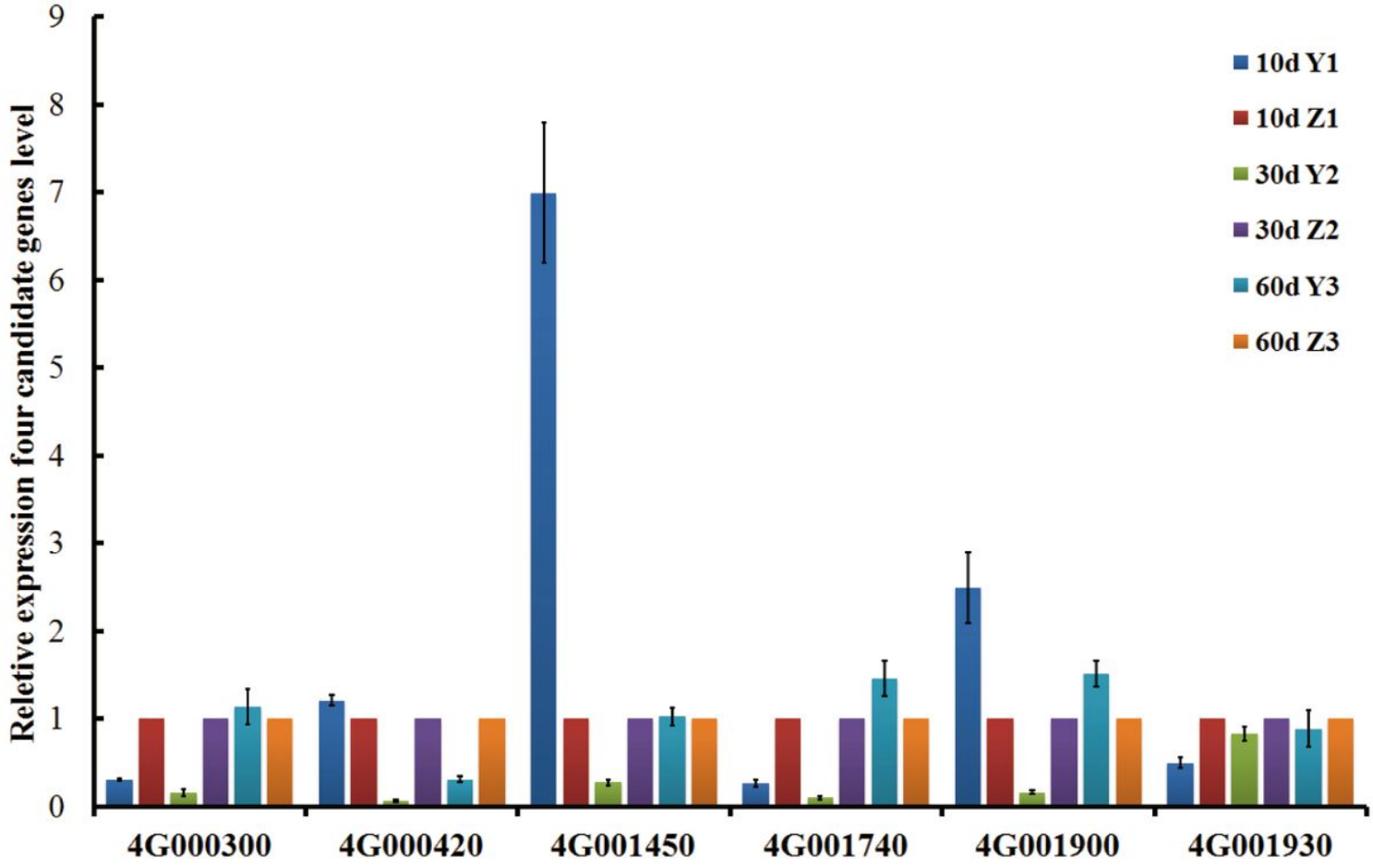

Figure 6

Relative expression levels of six candidate genes in lesion mimic mutant clalm and wild-type Zhengduanman watermelon. Data are presented as the mean of three independent measurements. Error bars represent the standard deviation of mean values.

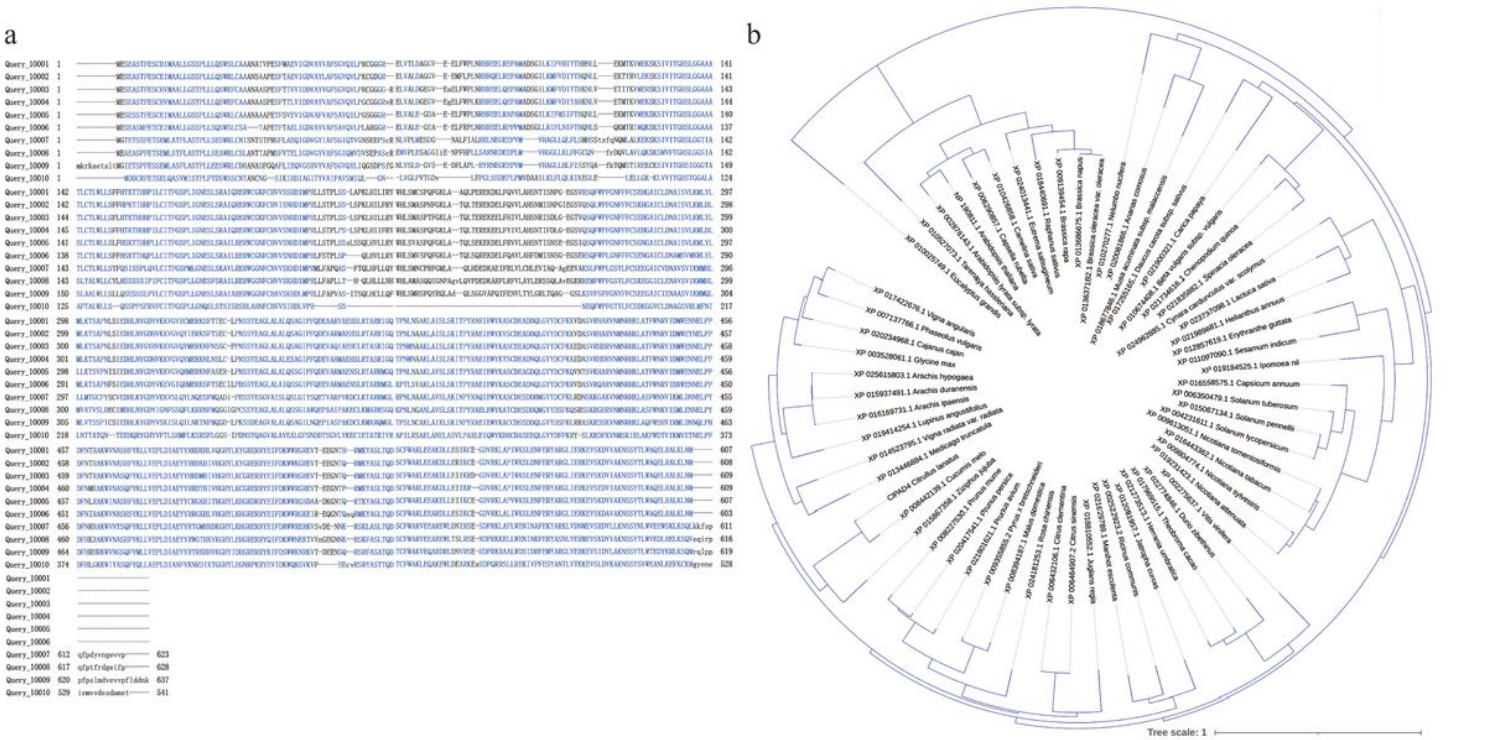

Figure 7

Bioinformatics characteristics of ClPAD4. a Results of Blast comparison of ClPAD4 proteins from various angiosperms. Query_10001 = Citrullus lanatus lipase-like PAD4 (Gene ID:ClCG04G001930); Query_10002 = Benincasa hispida lipase-like PAD4 (gene ID:LOC120072712); Query_10003 = Cucumis sativus lipase-like PAD4 (gene ID:LOC101222098); Query_10004 = Cucumis melo lipase-like PAD4 (gene ID:LOC103486086); Query_10005 = Cucurbita maxima lipase-like PAD4 (gene ID:LOC111465963); Query_10006 = Momordica charantia lipase-like PAD4 (gene ID:LOC111017842); Query_10007 = Quercus suber lipase-like PAD4 (gene ID:LOC112032821); Query_10008 = Ziziphus jujuba lipase-like PAD4 (gene ID:LOC107404877); Query_10009 = Tripterygium wilfordii lipase-like PAD4 (gene ID:LOC119990818); Query_10010 = Arabidopsis thaliana lipase-like PAD4 (gene ID:At3g52430). b Phylogenetic tree based on ClPAD4 in different organisms. The GenBank accession numbers are provided. The sequences are in Supplementary Material.

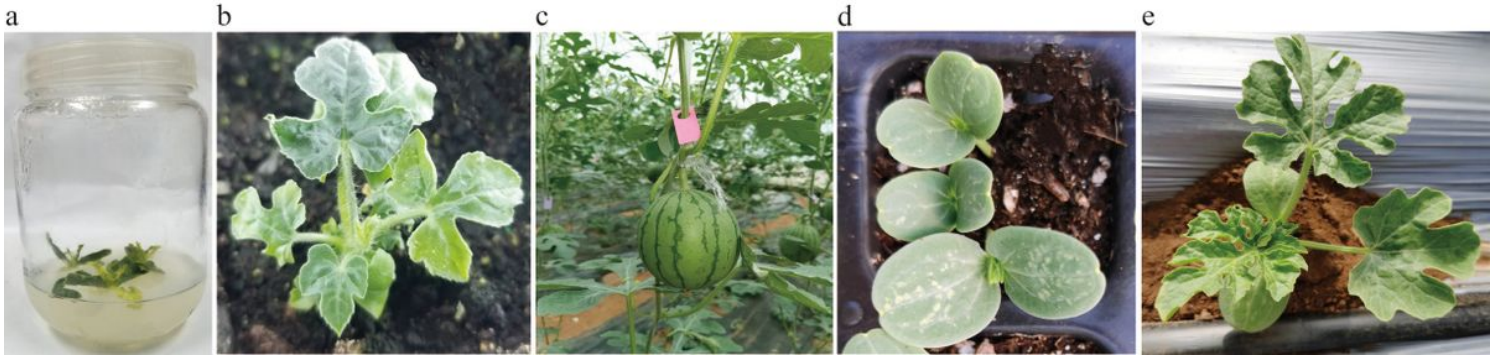

Figure 8

Growth stages of transgenic watermelon. (a) Adventitious shoots regenerated from cotyledons after 3 weeks. (b) Enlarged adventitious shoots. (c) T0 generation watermelon fruit. (d-e) 1-week-old (d) and 1-month-old (e) T3 generation seedlings.

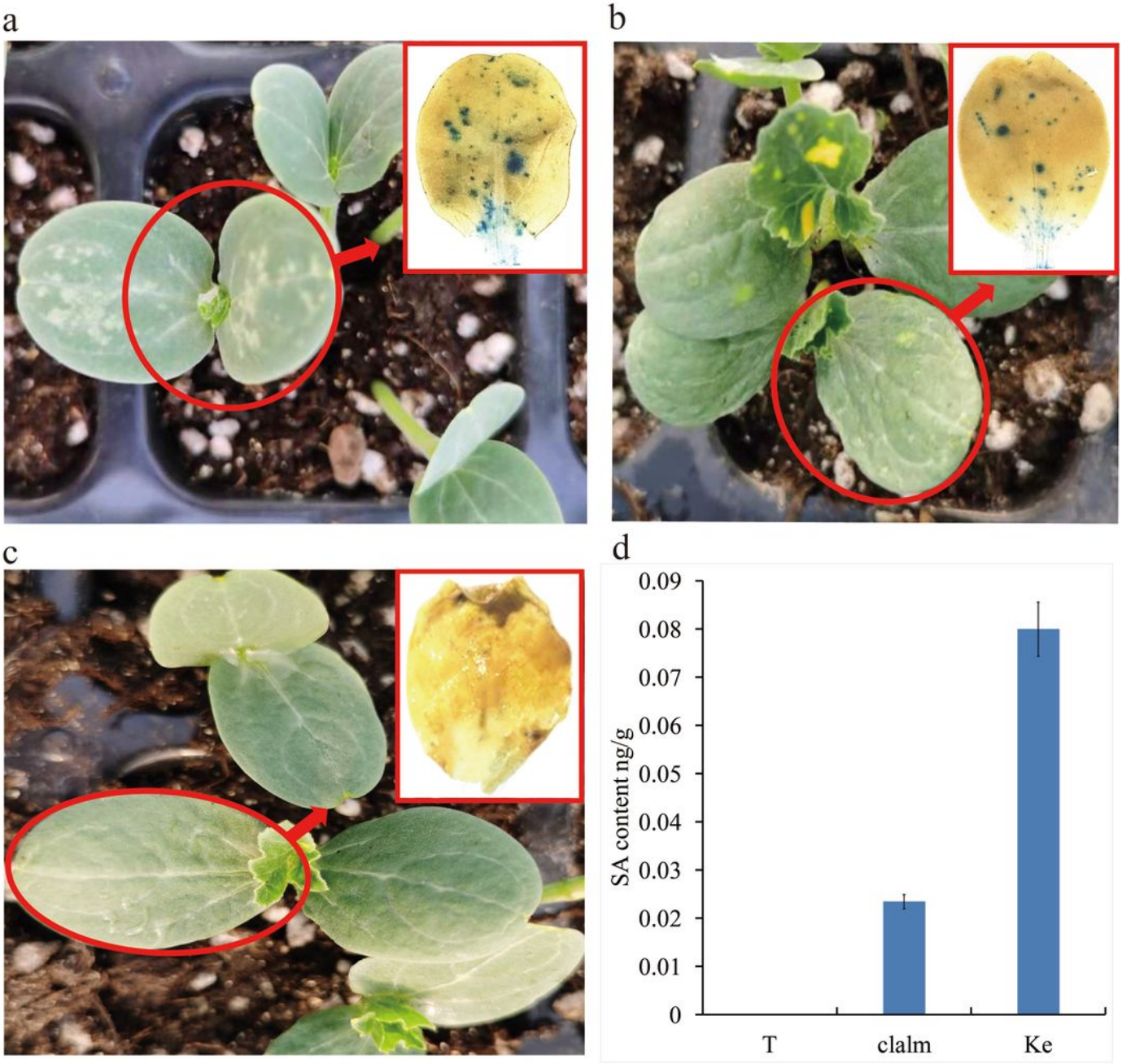

Figure 9

Results of histochemical staining of watermelon leaves. (a–b) Spotted leaves of transgenic (a), lesion mimic mutant clalm (b) and Kexi (c) watermelon stained with trypan blue. The inset shows leaves with

chlorotic lesions. d The SA content of the leaves.

Supplementary Files

This is a list of supplementary files associated with this preprint. Click to download.

- SupplementaryMaterial.pdf